The Role of Surface Deconstruction in the Autocatalytic Decomposition of Formate and Acetate on Ni(110)†

Ali R. Alemozafar and Robert J. Madix*

Department of Chemical Engineering, Stanford University, Stanford, California 94305-5025

Received: January 8, 2004; In Final Form: April 22, 2004

The adsorption of formate and acetate on the Ni(110) surface has been investigated with STM, LEED, TPRS, and XPS. At saturation coverage formate and acetate form a c(2 × 2) structure amid a pitted surface, which is suggestive of the incorporation of "added" Ni atoms into the c(2 × 2) structure. Heating the surface to 350 K to decompose the formate produces islands of step height, indicative of the release of Ni from the c(2 × 2) structure during HCOO decomposition. Upon further heating to 370 K the islands dissipate and p(4 × 1)-CO domains appear. Heating the acetate-covered surface affects a restructuring of the c(2 × 2) to scattered domains of a p(8 × 1) structure, which is attributed to acetate. Concomitant with this restructuring is the release of Ni to form islands of step height. Upon further heating the acetate decomposes to yield a p(4 × 5)-C covered surface. The present investigation adds further insight into the phenomena underlying the autocatalytic decomposition of formate and acetate. It is suggested that the added Ni in the formate structure facilitates the decomposition of formate into CO_2, H_2, and scattered Ni_x nuclei, which act as sites for further formate decomposition.

1. Introduction

In the early 1970s Falconer and Madix observed a surface kinetic explosion for the decomposition of formic acid (HCOOH) on the Ni(110) surface, characterized by a very narrow fwhm of individual temperature programmed reaction spectra (TPRS) associated with the decomposition of formate into CO, CO_2, and H_2.[1] This process displayed atypical kinetic behavior; the kinetic rate expressions suggested a vacancy-driven autocatalytic decomposition of the formate. In a follow-up investigation a similar autocatalytic decomposition for acetate on Ni(110) was found.[2]

At room temperature formic acid interacts dissociatively with the Ni(110) surface to yield gaseous H_2O and an adsorbed surface intermediate, which was revealed to be bidendate formate (HCOO),[3] and an HCO fragment that decomposes to CO and hydrogen. With increasing formic acid exposure, the formate displaces CO to yield a formate-covered surface.[4] With heating a fraction of the formate undergoes C−H bond cleavage to yield CO_2 and H_2, while the remainder proceeds via C−O bond cleavage to form CO and O. A fraction of the CO is believed to decompose into C and O, which have been shown to stabilize the formate.[5,6]

The autocatalytic nature of the decomposition of formate was previously explained by a reaction occurring at bare metal sites distributed randomly within formate islands.[1] As the reaction proceeded and the reaction products desorbed, the number of such sites increased, causing the reaction rate to accelerate. The rate of decomposition was accurately described by

$$\text{Rate} = -k(c/c_I)(c_I - c + fc_I) \qquad (1)$$

in which c is the formate surface concentration, c_I is the initial surface concentration, and f is the density of initiation sites. The autocatalytic decomposition of acetate is described equally well by eq 1.

The structure and orientation of the formate molecule were investigated previously by Jones et al.[7] using low energy electron diffraction (LEED) and high-resolution electron energy loss vibrational spectroscopy (HREELS). The adsorption of formate yielded a c(2 × 2) LEED pattern. EELS data and symmetry arguments were used to suggest that HCOO binds to the surface via its two oxygen atoms (bidentate) across short-bridge sites, with the plane of the molecule aligned along the [1$\bar{1}$0] azimuth. Nowicki et al.[8] arrived at similar findings in their X-ray photoelectron diffraction (XPD) spectroscopy investigation of acetate on Ni(110). The adsorption of CH_3COO yielded a c(2 × 2) structure at saturation coverage. Further analysis of the spectra led the authors to suggest a short bridge site binding configuration of the individual, bidendate acetate molecules within the c(2 × 2) structure.

The connection between the surface structure and the autocatalytic decomposition of the formate and acetate is not known. To gain further insight, a local assessment of the surface structures is required, which can most accurately be gained via scanning tunneling microscopy (STM), the advent of which has enabled numerous detailed, atomic-scale investigations of metal, metal-oxide, and semiconductor surfaces. Recent STM studies have elucidated the distribution of formate and acetate on the Cu(110)−p(2 × 1)-O surfaces.[9−11] Amid the p(2 × 1)-O covered surface formate adsorbs into structures with c(2 × 2), p(3 × 1), and p(4 × 1) periodicities.[9]

In this communication we present the results of our STM, LEED, TPRS, and XPS investigations of formate and acetate on the Ni(110) surface. The morphological changes to the surface structure following formic and acetic acid adsorption are suggestive of the incorporation of a stoichiometric quantity of Ni atoms into the carboxylate structures. With heating, the "added" Ni is released and is believed to facilitate the autocatalytic decomposition of formate and acetate.

† Part of the special issue "Gerhard Ertl Festschrift".

10.1021/jp0400061 CCC: $27.50
Published on Web 06/19/2004

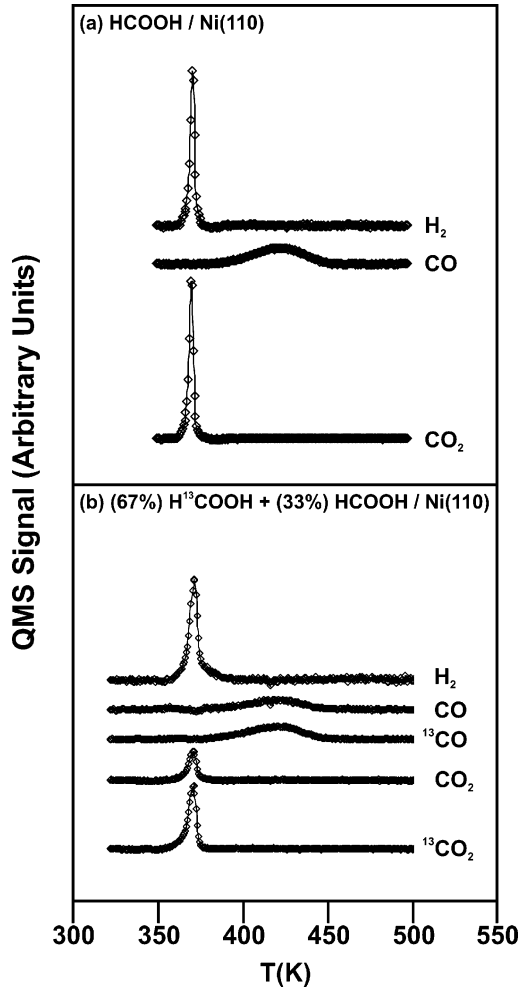

Figure 1. TPR spectra for saturation exposure (60 L) of (a) HCOOH on Ni(110) and (b) a 2:1 mixture of $H^{13}COOH$ and HCOOH on Ni(110). The CO and ^{13}CO peaks have been corrected for CO_2 and $^{13}CO_2$ cracking by the QMS ionizer using a scaling factor of 0.2, which was determined from saturation HCOOH TPRS like those shown (a) where CO at 360 K was ascribed to CO_2 cracking.[1]

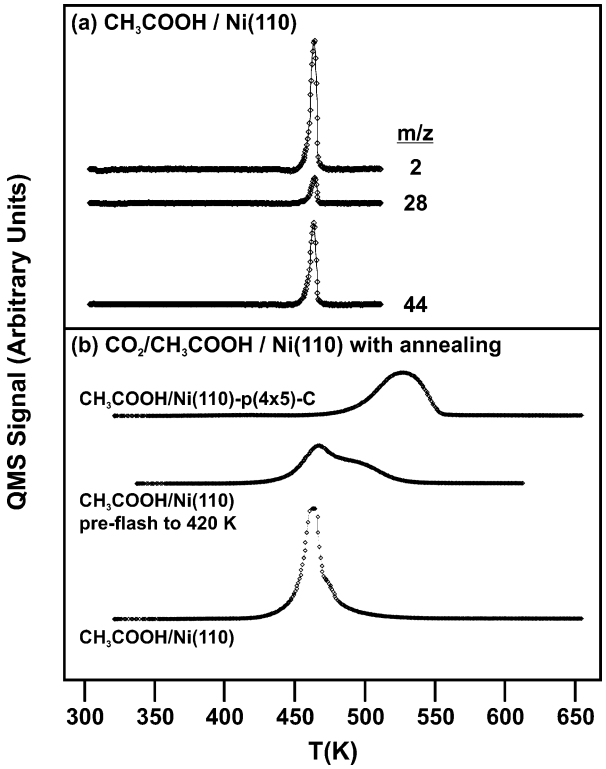

Figure 2. TPR spectra for saturation exposure (12 L) of (a) CH_3COOH on Ni(110) and (b) CH_3COOH on Ni(110) following annealing (1 K/s) to 420 K and a quench to room temperature. The $m/z = 28$ signal has not been corrected for CO_2 cracking by the QMS ionizer. Spectra taken following acetic acid exposure to a clean and a p(4 × 5)-C covered surface are shown in (b) for reference. The $m/z = 44$ signal is displayed in each case. The heating rates in (a) and (b) were 1 K/s and 2 K/s, respectively.

2. Experimental Section

Experiments were performed in an ultrahigh vacuum chamber equipped with STM, low energy electron diffraction (LEED), Auger electron spectroscopy (AES), and temperature programmed reaction spectroscopy (TPRS). Unless otherwise stated, a linear heating rate of 1 K/s was employed for all TPRS measurements. The chamber was equipped with a sputter ion gun and stainless steel gas dosers. The system exhibited a base pressure of 2×10^{-10} Torr following cleaning, which rose to approximately 5×10^{-10} Torr during experiments.

The homemade "Johnnie Walker" type STM uses RHK STM 100 control electronics and a Pt/Ir tip. The tip was prepared by field evaporation onto a gold foil ($\sim$ 3.9 μA, 15 min) prior to STM measurements. STM scan dimensions were calibrated using the Ni(110)−p(2 × 1)-O structure.[12]

The crystal was cleaned in a vacuum by three Ar^+ sputter (2 μA, 500 eV, 600 K, 10 min) and annealing (1050 K, 10 min) cycles, with the first anneal done in an oxygen atmosphere (1×10^{-7} Torr) to cleanse the surface carbon. Residual oxygen was removed via hydrogen treatment at 600 K followed by a final sputtering and annealing cycle. This cleaning procedure yielded a sharp p(1 × 1) LEED pattern. Within detectable limits ($\sim$ 4%), AES showed the surface to be devoid of sulfur, carbon, and oxygen impurities. The crystal could be cooled to 120 K with liquid nitrogen and heated to 1100 K by electron bombardment to the back of the crystal. A Chromel-Alumel thermocouple spot-welded to the back of the crystal was used to monitor the temperature. The ramp housing the crystal was allowed to thermally equilibrate for half an hour with the STM scan head prior to STM measurements.

Separate XPS and TPRS measurements were made in a second UHV system consisting of interconnected preparation and analysis chambers. The analysis chamber exhibited a base pressure of 2×10^{-10} Torr and was equipped with LEED optics, a Perkin-Elmer 04−548 dual anode X-ray source, an EA-10-plus hemispherical energy analyzer from SPECS, and a UTI 100c quadrupole mass spectrometer (QMS) used for TPRS measurements. The surface composition was probed with XPS using nonmonochromatic Mg Kα X-rays. The ionizer of the QMS was enclosed in a glass cap with a small hole facing the crystal surface. A computer coupled to the QMS was used to record TPR spectra. The preparation chamber reached a base pressure of 8×10^{-10} Torr and was equipped with a sputter ion gun and stainless steel gas dosers. The two chambers were isolated from each other during experiments.

In the XPS system the crystal was heated resistively via two W wires spot-welded to the back of the crystal. The temperature was monitored by a Chromel-Alumel thermocouple spot-welded to the back-edge of the crystal. The surface was cleaned by three sputter-anneal cycles, with the first anneal done in an O_2 atmosphere at 10^{-7} Torr. Residual oxygen was removed via hydrogen treatment at 600 K followed by a final sputtering and annealing cycle. Within detectable limits, XPS showed the surface to be devoid of sulfur, carbon, and oxygen impurities

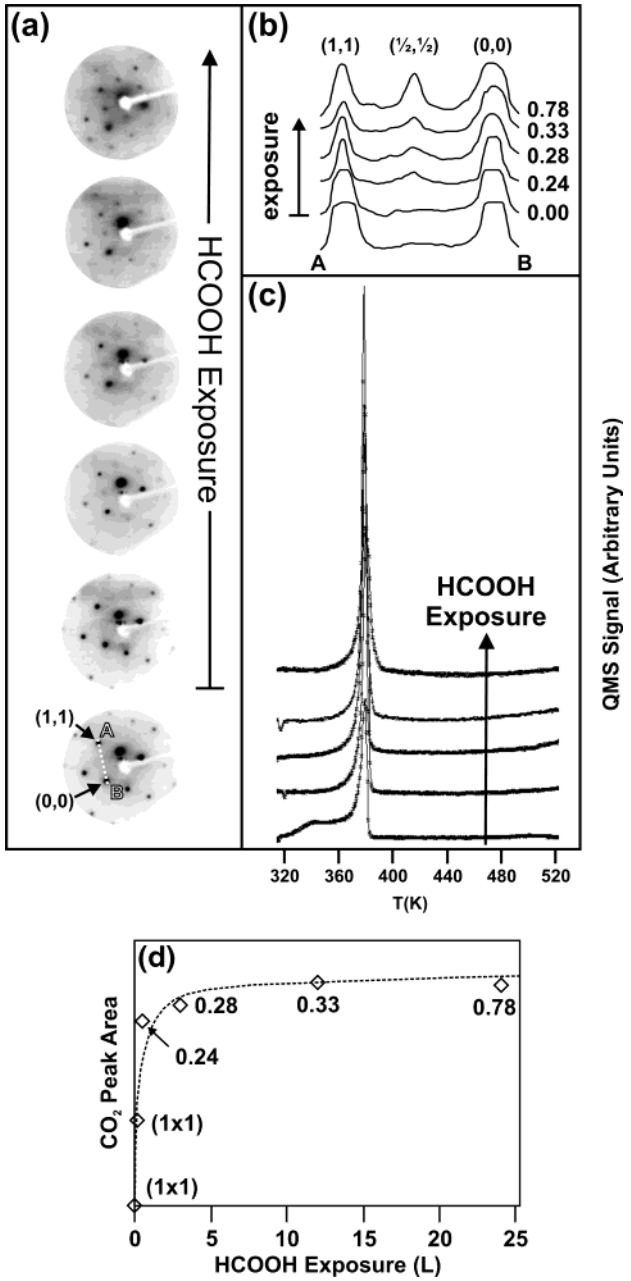

Figure 3. (a) LEED measurements, showing the development of the c(2 × 2)-formate structure with increasing formic acid exposure toward saturation (bottom to top). The (1 × 1) at the bottom was obtained following cleaning. The (0,0) and (1,1) spots of the (1 × 1) have been indicated in the bottom spectrum. The beam energy was ∼ 120 eV. (b) LEED spot intensity profiles accompanying the LEED patterns in (a). Profiles were taken along line AB, as shown in the bottom LEED pattern of (a). The ratio of the ($^1/_2$,$^1/_2$) peak to that of the most intense (1 × 1)—(0,0) or (1,1) spot—peak is displayed to the right of each profile. (c) $m/z = 44$ (CO_2) from temperature-programmed reaction of formate accompanying the LEED patterns in (a). (d) The increase in CO_2 peak area with formic acid exposure is concomitant with the appearance and intensification of the c(2 × 2) LEED pattern. The LEED profile peak ratios from (b) have been indicated. Formic acid was introduced via a needle doser directed at the face of the crystal. Exposures in Langmuir (L) have not been corrected for doser enhancement.

following the cleaning procedure. The photoelectrons were collected at the surface normal by the energy analyzer using a 25 eV pass energy. Binding energies were calibrated with respect to the Au 4f peak (84.00 eV) and referenced to the Ni($2p_{3/2}$) peak.

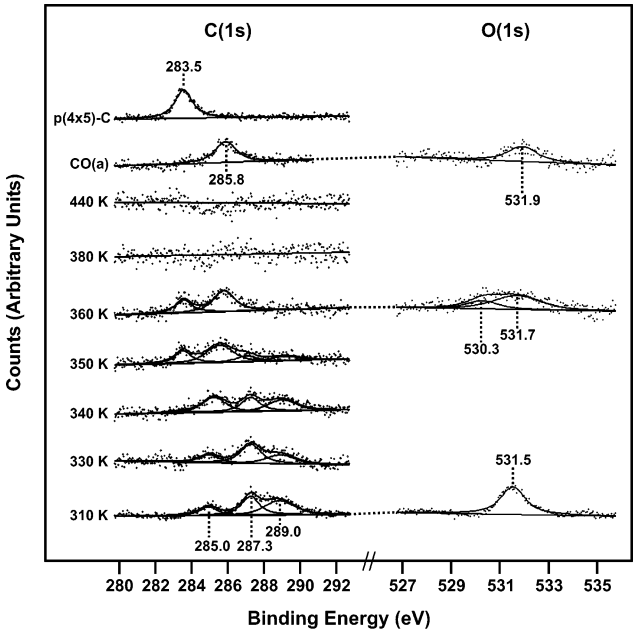

Figure 4. C(1s) and O(1s) XP-spectra showing the state of the formate-covered surface (saturation coverage) taken after annealing (2 K/s) to the indicated temperature and cooling (∼ 1 K/s) to 310 K. Deconvolutions of select C(1s) and O(1s) peaks appear with the raw data. The CO(a) and p(4 × 5)-C reference spectra were taken from surfaces prepared by CO(g) exposure (1 × 10^{-7} Torr) at 310 K and ethylene cracking at 550 K, respectively. Peak energies have been tabulated in Table 1.

The purity of the H_2(g) (Praxair, 99.98%), O_2(g) ($^{16}O_2$, Praxair, 99.999%), HCOOH(g) (Acros Organics, 99+%), H^{13}COOH (Aldrich, 99% formic acid; 67% ^{13}C, 33% ^{12}C), CH_3-COOH(g) (J. T. Baker, 99.9%), and C_2H_4(g) (Matheson, 99.999%) was monitored with the QMS during dosing. Formic and acetic acid were outgassed every day by freeze−pump−thaw cycles until a constant vapor pressure was obtained over the solid. Unless otherwise stated, all gases were dosed from the background. Exposures are reported in units of Langmuir (1 L = 10^{-6} Torr s).

3. Results and Discussion

3.1. TPRS Investigation. As expected, TPR-spectra of a formate-covered Ni(110) surface show reaction-limited CO_2 and H_2 desorbing in a narrow (fwhm ∼ 10 K), explosive peak centered at 360 K, followed by desorption-limited CO at 410 K (Figure 1a). Measurements are in good agreement with those performed previously by Falconer et al.[1,13]

TPRS measurements with isotopically labeled formic acid (H^{13}COOH) suggest that the desorption-limited CO observed in formate TPR-spectra (Figure 1a) is due to C−O bond cleavage of surface formate (Figure 1b). The TPD spectra show masses corresponding to those of CO_2, CO, and their ^{13}C isotopes, namely ^{13}CO and $^{13}CO_2$. This shows that the origin of CO during formate TPRS is HCOO and not solely CO from the background, which is in agreement with expectations.

The decomposition of acetate is marked by the reaction-limited evolution of CO_2, CO, and H_2 at 460 K (Figure 2a). The spectra shown are of a fully covered, saturated acetate overlayer. The peak temperatures for acetate decomposition are shifted up in temperature by approximately 100 K and slightly broadened (fwhm ∼ 15 K) relative to formate. This result is in good agreement with that observed previously by Falconer et al.[2] With heating the acetate undergoes C−H bond scission to

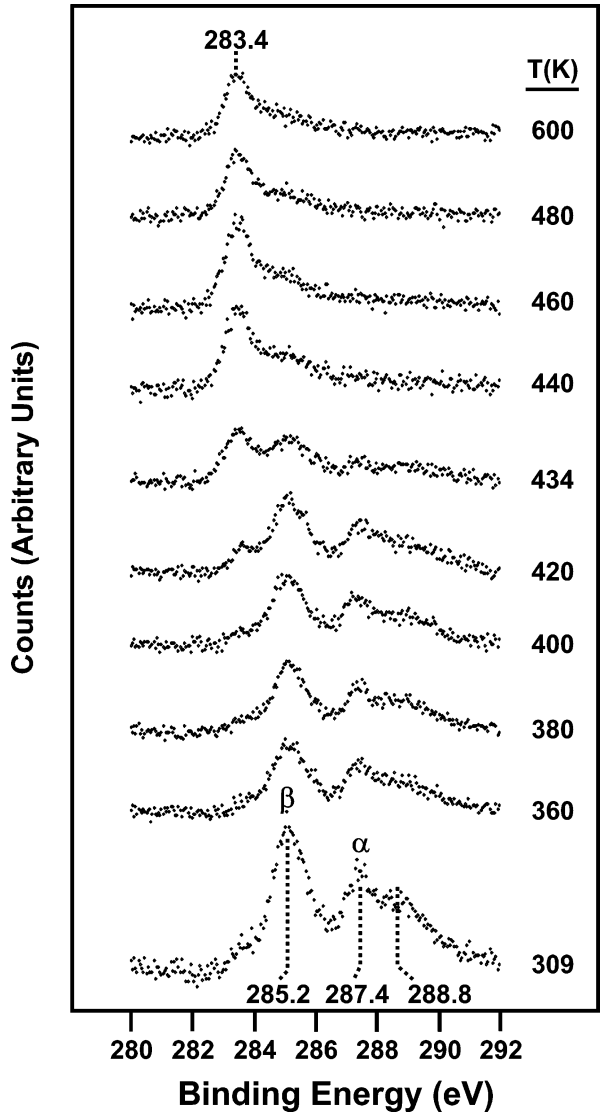

Figure 5. C(1s) XP-spectra of the acetate-covered surface (saturation coverage) taken after annealing (2 K/s) to the indicated temperature and cooling (~ 1 K/s) to 309 K. Peak energies have been tabulated in Table 1.

TABLE 1

	C	CO	CO_2	HCOO	CH_3COO
Ni(100)	284.75[14]	285.4[15]	-	-	-
Ni(110)	283.5	285.8	286.4[16]	287.3	α 287.4 β 285.2
Ni(111)	-	285.5[17]	-	-	-
Ru(001)	-	285.7[17]	-	-	-
O_2/Cu	-	-	-	287.5[18]	-
Fe(100)	-	-	-	288.3[19]	288.8[19]
Cu(110)	-	-	-	287.7[20]	α 288.2[21] β 285.0[21]
Ag(110)	-	-	-	-	α 287.2[22] β 284.1[22]

yield CO_2 and a CH_3 fragment, which rapidly decomposes to yield H_2 and surface carbon. Carbon has been identified by AES and further shown by STM (see below).

An interrupted flash of the acetate-covered surface to 420 K yielded a high temperature shoulder accompanying the explosive peak at 460 K (Figure 2b). By comparison to a TPD of acetate on a p(4 × 5)-C covered surface, this effect is ascribed to the build-up of carbon on the surface due to acetate decomposition. The peaks in acetate TPR-spectra behaved differently from those

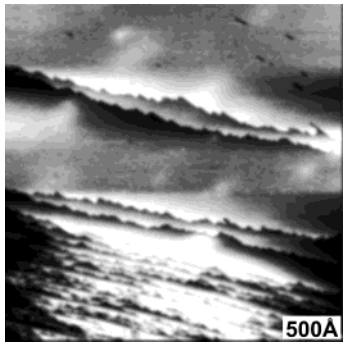

Figure 6. STM micrograph of the surface at 300 K following our cleaning procedure; the tunneling conditions were −98.7 mV and 0.57 nA.

for formate, which with increasing pre-flashing temperature decrease in intensity and shift to a lower temperature.[1]

3.2. LEED Investigation. LEED and TPR spectra show the evolution of the formate structure with increasing coverage (Figure 3). The formate LEED spectra are in agreement with those reported previously.[7] During LEED measurements the crystal was kept under the electron beam for approximately 30 s. A sharp p(1 × 1) LEED pattern (Figure 3a, bottom profile) was obtained following our cleaning procedure. With increasing formate coverage (bottom to top), centered ($^1/_2$, $^1/_2$) spots appeared and grew in intensity (Figure 3b). The LEED pattern following saturation exposure of formic acid (~ 60 L) was a c(2 × 2). TPR spectra taken immediately after the LEED measurements show a direct correlation between the height of the explosive peak and the development of the c(2 × 2) LEED pattern (Figure 3c). Only $m/z = 44$ (CO_2) peaks are shown. An increase in the CO_2 peak area with increasing formic acid exposure is concomitant with the appearance and intensification of the c(2 × 2) spots in LEED spectra (Figure 3d). With increasing formic acid exposure the low temperature shoulder disappeared and the 370 K explosive peak grew in intensity. These results suggest that the intensity of the autocatalytic decomposition of formate is dependent on the density of c(2 × 2)-formate islands.

The development of the acetate overlayer was qualitatively identical to that of formate. A saturation exposure (~ 12 L) of acetic acid yielded intense c(2 × 2) LEED spots.

3.3. XPS Investigation. Changes in the formate- and acetate-covered surfaces with temperature were characterized with XPS (Figures 4 and 5). The C1s peak energies from the present investigation (unreferenced entries) and previous work[14−22] are summarized in Table 1. C1s and O1s XP-spectra following the adsorption of formic acid are shown in Figure 4. Reference spectra for CO(a) and p(4 × 5)-C covered surfaces are shown for comparison. The C1s spectrum at 310 K exhibited features attributable to CO (285.0 eV), formate (287.3 eV), and a broad, high-energy peak at 289.0 eV that is believed to be a "shake up" in the final state of the formate photoemission.[22] The broad O1s peak at 531.5 eV is in good agreement with what has been observed for formate on Cu(110)[20] and Fe(100).[19] Following calibration with C1s XP-spectra obtained for a p(4 × 5)-C covered surface at 0.6 ML,[23] the coverage of CO and HCOO is estimated to be 0.119 ± 0.002 ML and 0.328 ± 0.008 ML, respectively. The 287.3 eV C1s formate peak is in good agreement with that previously observed at 287.5 eV for formate on an oxidized Cu(110) surface.[18] Assignment of the "shake up" peak to formate is supported by the fact that (with heating) its intensity attenuates together with the formate 287.3 eV peak. Similar satellite features have been observed for the chemi-

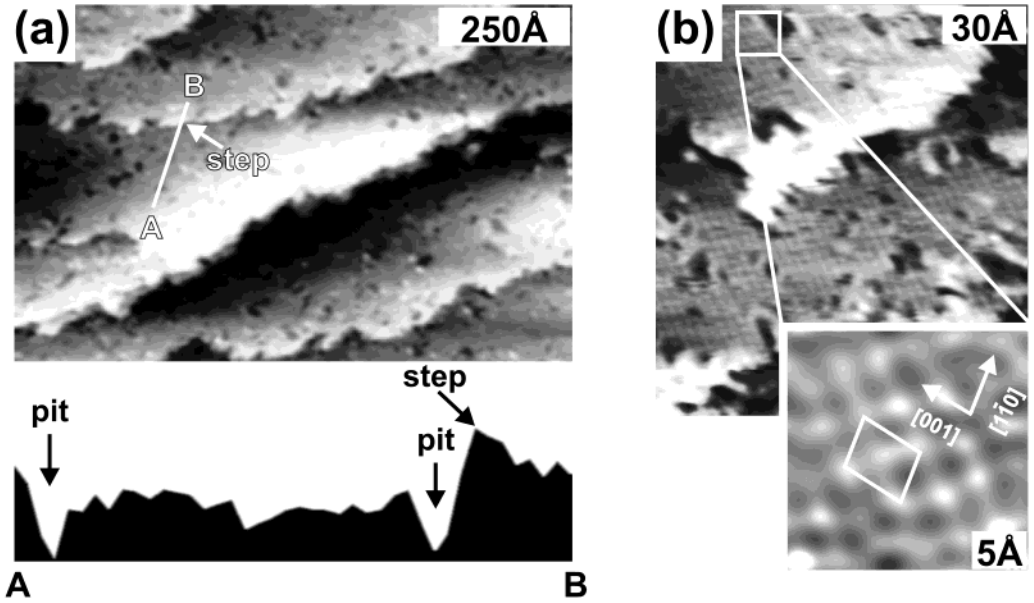

Figure 7. STM micrographs of the clean surface at 300 K following saturation exposure (60 L) of formic acid; the tunneling conditions were 0.67 V and 0.60 nA. The line scan (line AB) shows the pits to be of step depth. (b) Magnification of the surface in (a); the tunneling conditions were 0.63 V and 0.60 nA. An enlargement of the c(2 × 2) formate structure is shown in the inset.

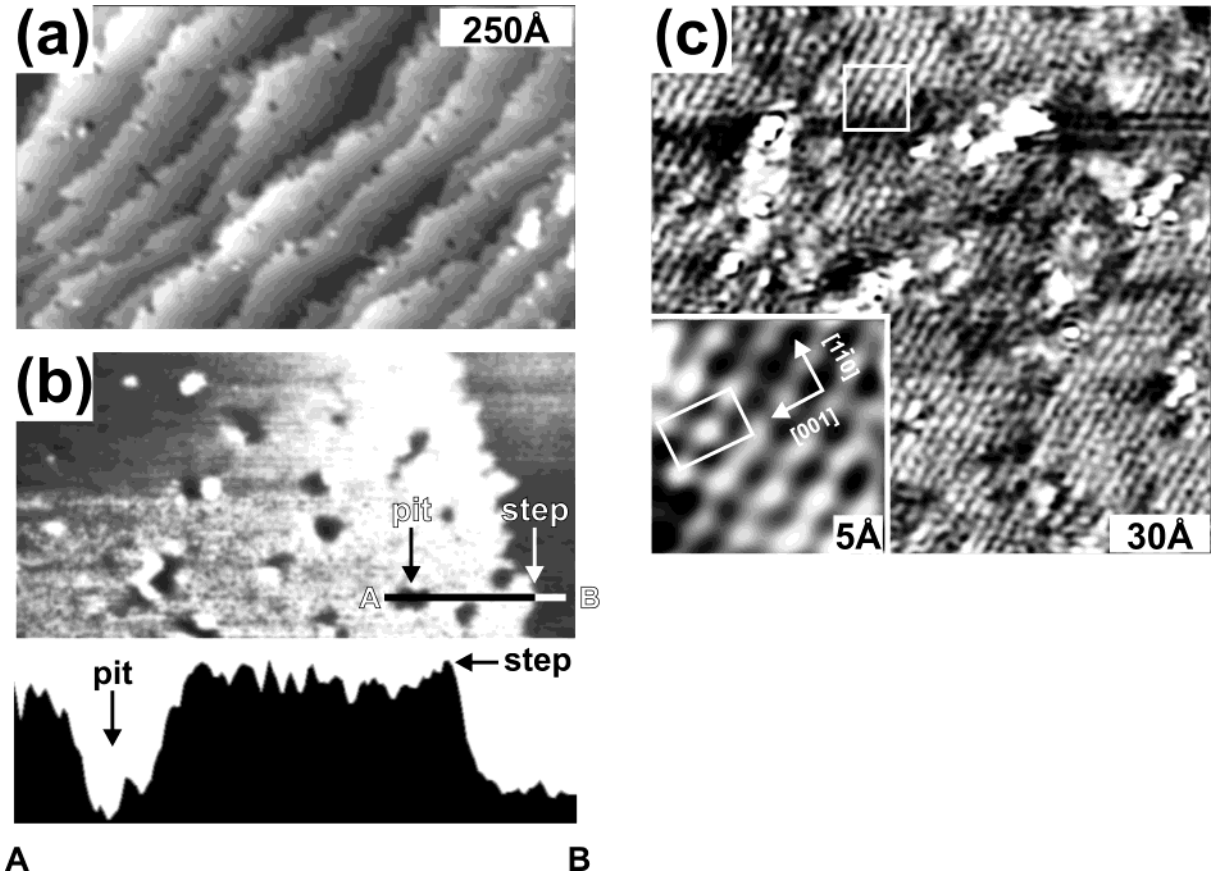

Figure 8. STM micrographs of the clean surface at 300 K following saturation exposure (12 L) of acetic acid; the tunneling conditions were 460 mV and 0.48 nA. The line-scan (line AB) shows the pit to be of step depth. (b) Magnification of the surface in (a) and the accompanying line-scan (line AB), which shows the pits to be of step depth; the tunneling conditions were −299 mV and 0.40 nA. (c) Scan of the surface in close vicinity to that in (b), showing the c(2 × 2) acetate structure (inset); the tunneling conditions were −299 mV and 0.40 nA. The crystal was reoriented between Figures 7 and 8.

sorption of CO,[24,25] N_2,[26] and C_2H_2[22] on metal surfaces. They have been explained in terms of the final state relaxation of the adsorbed species.[27] Heating the formate-covered surface effected an attenuation of the HCOO C1s peak and a broadening of the O1s peak. The peak energies at 360 K are indicative of CO (0.19 ML), carbon (0.12 ML), and oxygen (0.19 ML) adsorption. Upon further heating CO desorbed from the surface while carbon and oxygen went to the subsurface.[1] From the initial HCOO

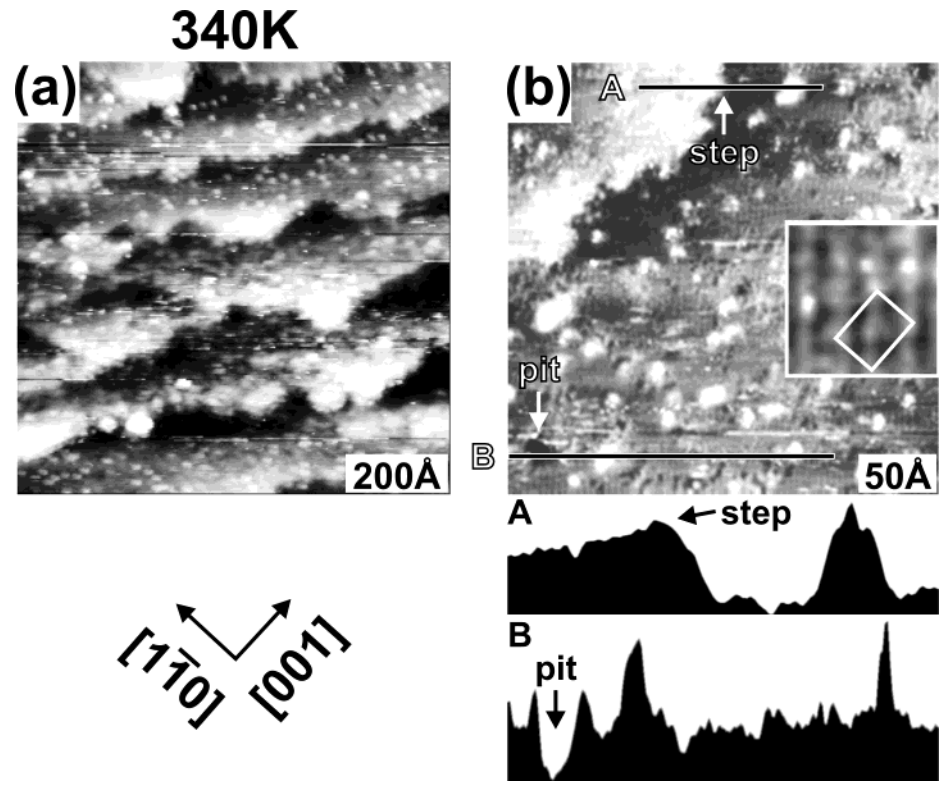

Figure 9. STM micrograph of the formate-covered surface resulting from heating to the indicated temperatures; the tunneling conditions were −426 mV and 0.60 nA (set-point). (a) Large scale and (b) small scale scans of the surface at 340 K, showing bright protrusion of step height (line scan A) and pits of step depth (line scan B) amid domains of the c(2 × 2) structure, which is better resolved in the enlargement (right image, inset).

coverage and the CO and C coverage following formate decomposition, the selectivity toward C−H bond cleavage is estimated to be 0.75.

X-ray photoelectron spectra taken following the adsorption of acetate (Figure 5) showed distinct peaks at 287.4 and 285.2 eV, which are ascribed to photoemission from the carboxyl (α) and methyl (β) carbons of CH_3COO(a). Additionally there is a broad "shake up" shoulder at 288.8 eV accompanying the acetate α peak. The acetate coverage is 0.324 ± 0.006 ML The ratio of areas of the CH_3COO(a) β peak to the sum of the α and "shake up" peaks is 1:1. The energy difference between the α and β peaks (2.3 eV) is slightly lower than what has been reported for acetate on Ag(110) and Cu(110), for which the peak-to-peak separation was 3.1 and 3.2 eV, respectively. This discrepancy may be due to the presence of the shake up shoulder, which is absent on Ag(110) and Cu(110). With heating the acetate peaks attenuated, and a new, low energy peak appeared at 283.4 eV that is attributed to carbidic carbon (Table 1). The decomposition of acetate was complete by 460 K, giving rise to a carbon coverage of 0.31 ML. This value is close to the initial acetate coverage, as is expected, since the decomposing CH_3COO will leave behind carbon after losing its CH_3- moiety via

$$CH_3COO(a) \rightarrow CO_2(g) + 3/2\ H_2(g) + C(a) \qquad (2)$$

3.4. STM Investigation. *3.4.1. c(2 × 2) Formate and Acetate*. An STM scan characteristic of the surface following our cleaning procedure (Figure 6) shows bunched steps and large terraces hundreds of angstroms wide in the direction of the [001] vector. The [1$\bar{1}$0]-oriented pits on the terrace in the upper part of the image result from the formation of mobile Ni_xH_y clusters.[28]

Morphological changes to the surface structure accompanying formate adsorption are suggestive of the incorporation of Ni

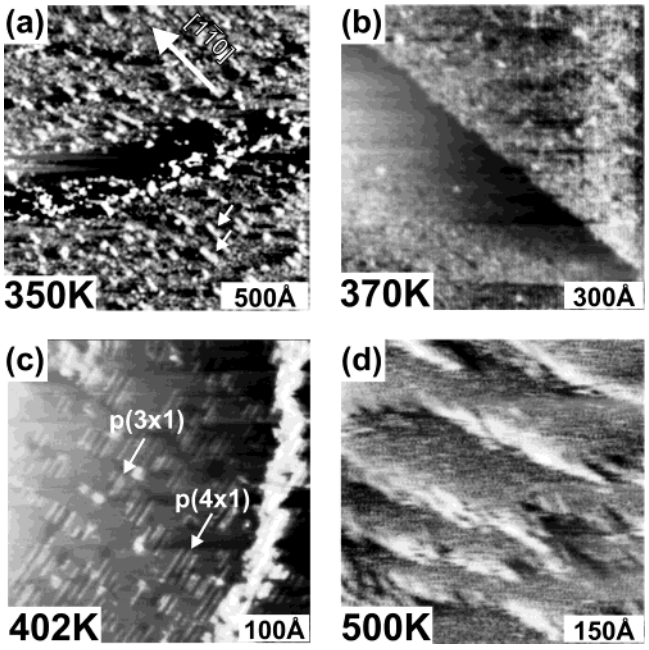

Figure 10. Scans of the surface in Figure 9 after heating to (a) 350 K, (b) 370 K, (c) 402 K, and (d) 500 K; the tunneling conditions were −426 mV and 0.60 nA (set-point).

atoms into the formate structure. An STM scan representative of the surface following a saturation exposure of formic acid is shown in Figure 7a. Roughened steps and pits of monatomic step depth are observed. At higher magnification (Figure 7b) scattered pits amid large c(2 × 2)-formate domains are observed. The c(2 × 2) structure could not be imaged at lower coverages, presumably due to the mobility of the formate. The pits, which are of step depth, cover approximately 33% of the surface at locations far from steps. No structures are observed within the

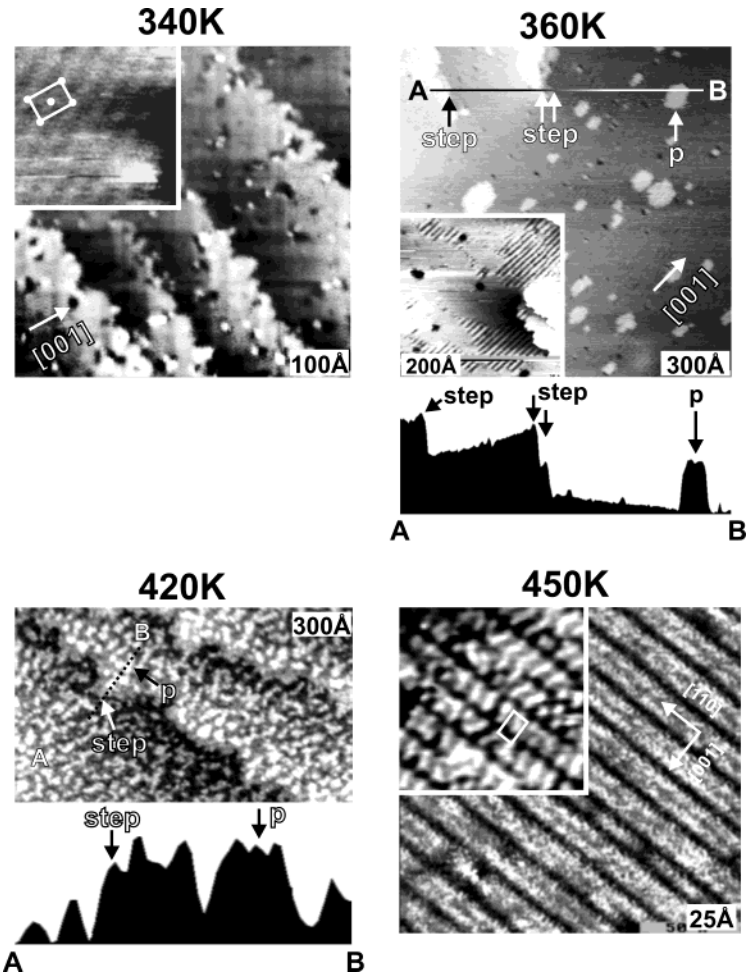

Figure 11. STM micrographs of the acetate-covered surface at the indicated temperatures. The tunneling conditions were −100 to −400 mV and 0.60 nA (set point); 450 K frame inset, 477 mV and 0.59 nA. The c(2 × 2)-acetate structure is shown in the inset of the 340 K frame; white circles have been included to accentuate the c(2 × 2) structure. The inset to the 360 K frame is a magnification of the surface showing p(8 × 1) rows. The line scans accompanying the 360 and 420 K frames, lines AB, show the plateaus (p) to be of step height. The inset to the 450 K frame shows a p(4 × 5)-C reference structure, prepared via ethylene cracking at 550 K.

pits, which is similar to what was observed for SO_2 on Cu(110).[29] Assuming the local c(2 × 2)-formate coverage to be 0.5 ML and that there is no formate within the pits, the overall surface coverage of Ni incorporated in the c(2 × 2) structure is estimated to be 0.67 · 0.5 = 0.33 ML (33%), which is equal to the formate coverage estimated via XPS measurements (see the XPS investigation). This suggests that a stoichiometric quantity of Ni is incorporated into the formate structure, or

$$\mathrm{HCOOH(g) + Ni(s) \rightarrow HCOO{-}Ni(a) + {}^1/_2\, H_2(g)} \quad (3)$$

Structurally the adsorption of acetate is identical to that of formate (Figure 8a). A saturation exposure of acetic acid yielded a pitted surface (Figure 8b) with the dominant structure being c(2 × 2)-acetate (Figure 8c), in agreement with the observed c(2 × 2) LEED pattern and previous XPD results (see the Introduction). The pit coverage at locations on terraces far from step edges is 0.33 ML, which is equal to the acetate coverage estimated via XPS. This result suggests that the stoichiometric ratio between acetate and the added Ni is also one-to-one, or

$$\mathrm{CH_3COOH(g) + Ni(s) \rightarrow CH_3COO{-}Ni(a) + {}^1/_2\, H_2(g)} \quad (4)$$

Pit formation following formic and acetic acid exposure is one of many cases of topographic nanorestructuring, whereby the interaction between an adsorbate and the metal surface results in changes to the surface morphology at the nanometer scale.[29] The removal of metal atoms from the surface and subsequent incorporation into the adsorbate structure results in pits, and has also been observed for NO_2/Ag(110)−p(2 × 1)-O[30] and SO_2/Cu(110).[31] Conversely, the release of metal atoms during reaction can precipitate metal islands, as is the case for NH_3/Ag(110)−p(2 × 1)-O,[32] H_2/Ni(110),[28] and SO_2/Ag(110)−p(2 × 1)-O.[33] While reasons behind such surface restructuring are not understood, it is clear that the (110)-oriented metal surfaces studied thus far are more dynamic in their reactions than has been previously imagined.[34]

Morphological changes to the surface structure were also observed by Silva et al.[35] in their STM investigation of formate on Cu(110). In their work, the clean Cu(110) surface was exposed to formic acid followed by exposure to oxygen to pin the mobile formate into structures observable by STM. On terraces, formate arranged into structures displaying p(3 × 1) and p(4 × 1) periodicities, and at step edges it arranged into c(2 × 2) structures. Compression of formate into a local c(2 × 2) structure near step edges effected a "sawtooth" restructuring of the steps. This phenomenon was believed to be due to a decrease in the repulsive interactions of formate near step edges, which acts as a driving force for the sawtooth restructuring. Similar surface restructuring was observed for the adsorption of benzoate[36] and acetate[37] on Cu(110).

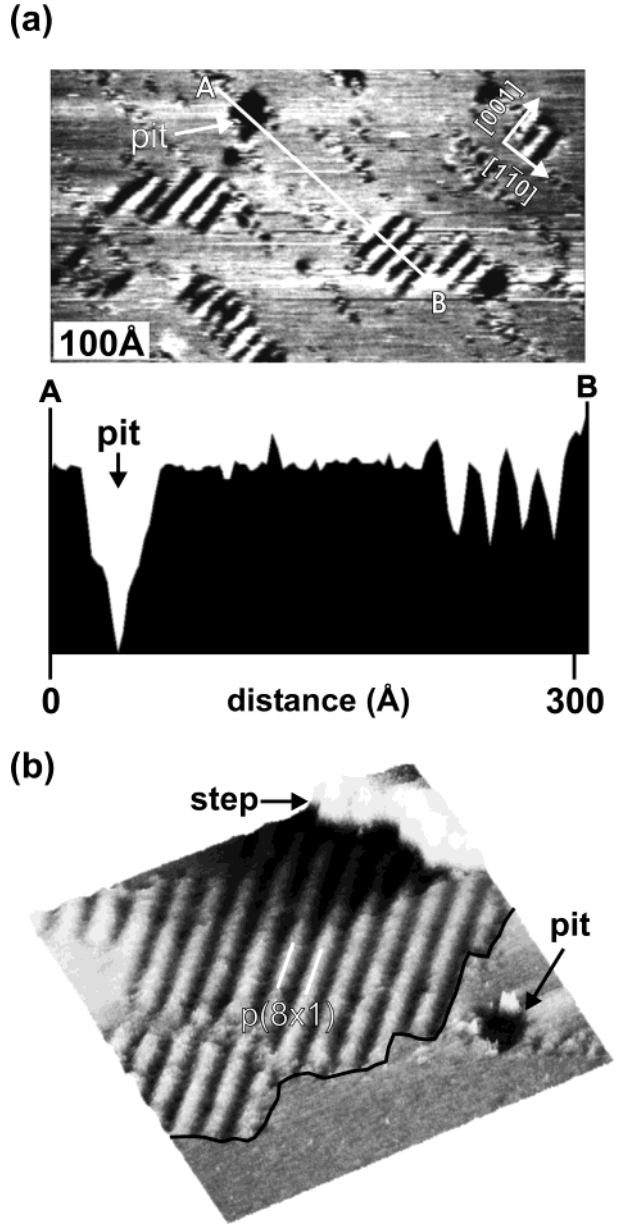

Figure 12. STM scans of (a) the p(8 × 1) structure following anneal (1 K/s) of the c(2 × 2)-acetate covered surface to 360 K; the tunneling conditions were −98.5 mV and 0.53 nA. The line scan (line AB) shows the depressions between the rows to be shallower than the pit (arrow), which is of step depth. (b) A three-dimensional scan of the p(8 × 1) structure; the tunneling conditions were −271 mV and 0.38 nA. The boundary between the p(8 × 1) and areas of the unresolved surface has been indicated.

3.4.2. Evolution of the Formate-Covered Surface with Temperature. Changes in the state of the formate-covered surface with increasing temperature are shown in Figure 9. The c(2 × 2)-formate covered surface was initially obtained via saturation exposure (∼ 60 L background) at 320 K followed by annealing to 340 K at 1 K/s, at which temperature the scan head and crystal assembly were allowed to thermally equilibrate for 30 min. A small temperature difference between the STM and the crystal produced thermal drift, which was mitigated by taking rapid scans (2 s/frame) of the surface.

The surface at 340 K consisted of pits of step height, bright (unresolved) features (Figure 9a), and domains of the c(2 × 2) structure (Figure 9b). The bright features, which are of monatomic step height (Figure 9b, line scan A), are interpreted as islands of Ni atoms that agglomerated during decomposition of a fraction of the formate overlayer. Heating to 350 K at 0.01 K/s effected an increase in the density of Ni islands (Figure 10[1$\bar{1}$0](g) from the Ni_xH_y-covered Ni(110) surface.[28] This result supports the claim that Ni was initially incorporated into the formate structure. The c(2 × 2) structure was not observed on this "roughened" surface. With further heating the Ni islands dissipated to fill-in the pits. The surface at 370 K was smoother, with fewer islands than the surface at a lower annealing temperature. Continued heating to 402 K affected the appearance of rows (white arrow) oriented along the [00$\bar{1}$] direction and spaced three to four lattice units along the [1$\bar{1}$0] azimuth. Since the registry in the direction of the [001] vector was not resolved, we tentatively assign these as p(3 × 1) and p(4 × 1) structures. The p(3 × 1) structure is ascribed to the low-coverage, p(3 × 1)-O structure imaged previously by Eierdal et al.[38] The p(4 × 1) periodicity is in agreement with what was observed previously for low-coverage CO.[39] The appearance of these features is consistent with our XPS measurements, which suggested the decomposition of a fraction of the formate into CO and O (Figure 4). Continued heating (0.1 K/s) beyond the CO desorption temperature (T_p = 420 K) to 500 K affected the disappearance of the p(3 × 1) and p(4 × 1) structures (500 K frame). The surface at 500 K exhibited a p(1 × 1) LEED pattern.

3.4.3. Evolution of the Acetate-Covered Surface with Temperature. Changes in the state of the acetate-covered surface with temperature are shown in Figure 11. Changes to the surface structure are nearly identical to those observed for formate (Figure 9), though there are differences, since the decomposition of acetate yields carbon. Initially, the acetate-saturated surface was obtained via exposure (12 L) of acetic acid at room temperature, followed by a 1 K/s anneal to 340 K, at which temperature the crystal and STM were allowed to thermally equilibrate for 30 min. The surface prepared in this manner displayed pits of monatomic step depth and domains on the terraces that were resolved at higher magnification to be comprised of the c(2 × 2)-acetate structure (340 K frame, inset). Annealing to 360 K (0.1 K/s) yielded a "p(8 × 1)" structure and Ni islands of step height (360 K frame, line scan). The appearance of Ni islands may be due to a restructuring of the acetate structure with heating (see below). Further annealing to 420 K effected a disordering of the surface structure and an increase in the concentration of Ni islands of monatomic step height (line scan). The p(8 × 1) rows were not observed at temperatures of 420 K and above. No structures on top of the Ni islands were resolved. Continued annealing to 450 K yielded a p(4 × 5) structure, consistent with the p(4 × 5) LEED pattern observed for this surface. By comparison to the p(4 × 5)-C obtained via ethylene cracking at 550 K (450 K frame, inset), this new structure is attributed to carbon from the decomposition of acetate. The p(4 × 5)-C structure is in agreement with what was observed previously by Besenbacher et al.[23]

The structures imaged following anneal of the acetate-saturated surface to 360 K consisted of rows five lattice units wide (along [1$\bar{1}$0]), separated by depressions that are three lattice units wide, or a "p(8 × 1)" structure (Figure 12a, b). From the line scan (Figure 12a) it is clear that the depressions between the thick rows of the p(8 × 1) structure are not of step depth. XPS measurements of a surface prepared in this manner revealed C1s features attributable solely to acetate (see the XPS section). Therefore, we interpret the p(8 × 1) structure as a restructing of the c(2 × 2) structure, which in turn forms scattered islands.

3.5. 2 D Structure and Role of Added Ni in Formate Decomposition. A two-dimensional model consistent with this work and previous measurements of formate and acetate on the

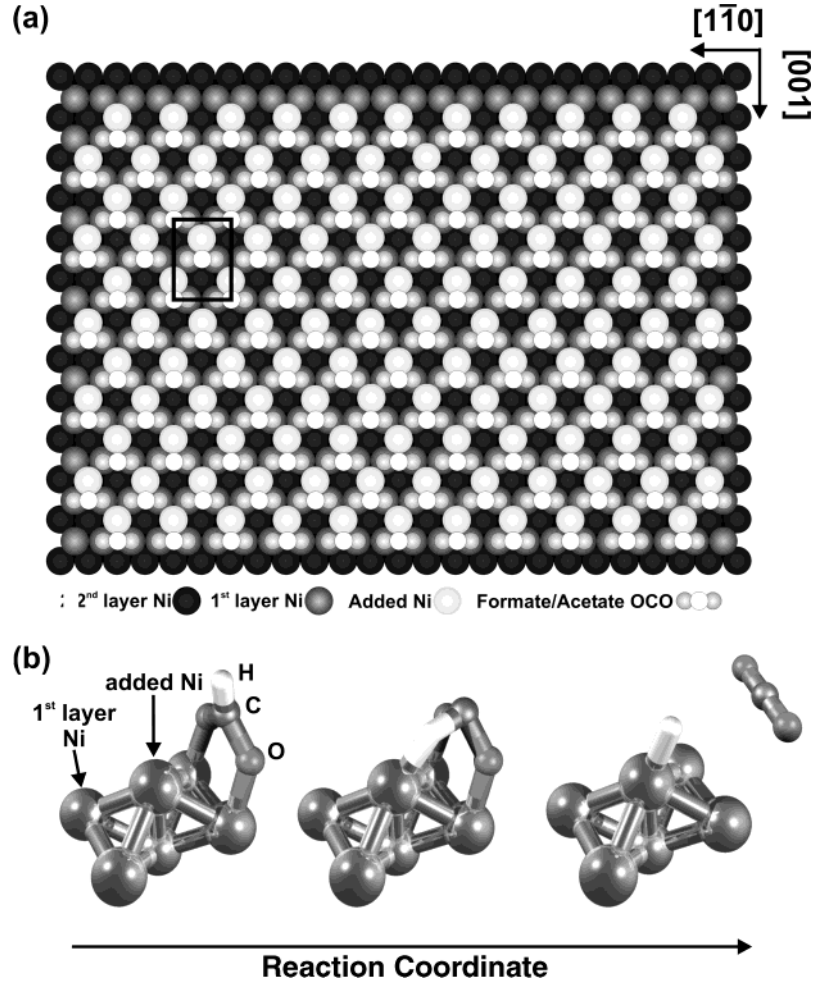

Figure 13. (a) Two-dimensional model showing the c(2 × 2) formate/acetate structure. (b) Three-dimensional representation of a reaction sequence between formate (HCOO) and an "added" Ni atom. The interaction between the HCOO and the "added" Ni atom may facilitate the decomposition of formate to CO_2(g) and Ni−H.

Ni(110) surface is shown in Figure 13a. The OCO fragment corresponds to that of formate or acetate. Both molecules have a bidentate short-bridge site binding configuration.[3,8]

The XPD investigation[8] of acetate on the Ni(110) surface suggested that the molecule tilts along the direction of the [001] vector. Similarly, a tilting of the formate molecule was used to explain the additional normal modes observed in the vibrational spectra of formate on Ni(110).[3] A previous investigation of hydrogen adsorption on Ni(110) is suggestive of the existence of mobile Ni_xH_y at room temperature.[28] Figure 13b shows a hypothetical reaction sequence in which formate interacts with an adjoining Ni atom. This interaction, which is most likely via the OCO π system of formate, effects a tilting of the formate toward the added Ni, which in turn positions the formate C−H bond to access the transition state for C−H bond cleavage. As the reaction proceeds, the concerted cleavage of the C−H bond and formation of the Ni−H bond yields CO_2. The Ni−H moieties subsequently recombine via

$$2\text{Ni}-\text{H(a)} \rightarrow \text{H}_2\text{(g)} + 2\text{Ni(a)} \qquad (5)$$

The Ni released in this process agglomerate into islands of step height, or plateaus (Ni_x).

The present investigation permits an alternative explanation for the autocatalytic decomposition of formate. Previously Falconer et al.[1] ascribed the autocatalytic decomposition of formate to vacancies, or unoccupied sites, within the formate structure. A mathematically equivalent explanation is that added Ni atoms released by the decomposition, as well as the configuration of the surface species in the c(2 × 2) structure, collectively mediate the autocatalytic decomposition of formate.

Previous TPRS measurements showed a decrease in the activation barrier to formate decomposition following interrupted flashes to temperatures below the explosive peak.[1] In the present investigation, island formation was observed following annealing of the c(2 × 2)-formate covered surface to 350 K (Figure 7). One possible structural explanation for the autocatalytic decomposition of formate is that it may occur at coordinatively unsaturated step edges of the Ni plateaus, which appear and accumulate with annealing. The availability of "free" Ni at these sites may affect the formation of a transition state involving more than one Ni interacting with formate.

Summary

The adsorption of formate and acetate on the Ni(110) surface has been investigated with STM, LEED, TPRS, and XPS. The results of the present investigation are summarized as follows:

(1) The adsorption of formate produces a c(2 × 2) LEED pattern that grows sharper with formic acid exposure. The development of the c(2 × 2) LEED pattern parallels the intensification of the explosive peak in formate TPR-spectra.

(2) XPS and STM results suggest that a stoichiometric quantity of Ni is incorporated into the c(2 × 2) formate and acetate structures.

(3) Annealing the formate-covered surface to 350 K effects the disappearance of the c(2 × 2) structure and the formation

of Ni islands (i.e. surface roughening). Upon further annealing the islands dissipate and p(3 × 1) and p(4 × 1) structures, attributable to low-coverage oxygen and CO, respectively, appear.

(4) Annealing the acetate-covered surface to 360 K effects a restructuring of the c(2 × 2) to domains of a p(8 × 1)-acetate structure and scattered Ni islands. No CO is observed on this surface. With heating to 400 K, the p(8 × 1) structures disappear and the Ni island density increases. Continued heating to 450 K produces a p(4 × 5)-C covered surface.

(5) The tilting of the formate and acetate is suggested as resulting from an interaction between the formate and acetate, and the added Ni in the c(2 × 2) structure.

(6) The autocatalytic decomposition of formate, which was originally proposed to be vacancy driven, is believed to be facilitated by precipitation of islands of Ni_x that increase in concentration during formate decomposition.

Acknowledgment. We are grateful to the National Science Foundation (NSF CHE 0209546) for support of this work.

References and Notes

(1) Falconer, J. L.; Madix, R. J. *Surf. Sci.* **1974**, *46*, 473.
(2) Madix, R. J.; Falconer, J. L.; Suszko, A. M. *Surf. Sci.* **1975**, *54*, 6.
(3) Madix, R. J.; Gland, J. L.; Mitchell, G. E.; Sexton, B. A. *Surf. Sci.* **1983**, *125*, 481.
(4) Haq, S.; Love, J. G.; Sanders, H. E.; King, D. A. *Surf. Sci.* **1995**, *325*, 230.
(5) McCarty, J.; Madix, R. J. *J. Catal.* **1975**, *38*, 402.
(6) Johnson, S. W.; Madix, R. J. *Surf. Sci.* **1977**, *66*, 189.
(7) Jones, T. S.; Ashton, M. R.; Richardson, N. V. *J. Chem. Phys.* **1989**, *90*, 7564.
(8) Nowicki, M.; Emundts, A.; Werner, J.; Pirug, G.; Bonzel, H. P. *Surf. Rev. Lett.* **2000**, *7*, 25.
(9) Haq, S.; Leibsle, F. M. *Surf. Sci.* **1997**, *375*, 81.
(10) Bennett, R. A.; Poulston, S.; Bowker, M. *J. Chem. Phys.* **1998**, *108*, 6916.
(11) York, S. M.; Haq, S.; Kilway, K. V.; Phillips, J. M.; Leibsle, F. M. *Surf. Sci.* **2003**, *522*, 34.
(12) Besenbacher, F.; Norskov, J. K. *Prog. Surf. Sci.* **1993**, *44*, 5.
(13) Falconer, J. L.; Madix, R. J. *Surf. Sci.* **1975**, *48*, 393.
(14) Akhter, S.; White, J. M. *Surf. Sci.* **1987**, *180*, 19.
(15) Belton, D. N.; Schmieg, S. J. *J. Vac. Sci. Technol., A* **1990**, *8*, 2353.
(16) Illing, G.; Heskett, D.; Plummer, E. W.; Freund, H.-J.; Somers, J.; Lindner, T. *Surf. Sci.* **1988**, *206*, 1.
(17) Wurth, W.; Schneider, C.; Treichler, R.; Umbach, E.; Menzel, D. *Phys. Rev. B* **1987**, *35*, 7741.
(18) Ayyoob, M.; Hegde, M. S. *J. Chem. Soc., Faraday Trans.* **1986**, *182*, 1651.
(19) Benziger, J. B.; Madix, R. J. *J. Catal.* **1980**, *65*, 49.
(20) Bowker, M.; Madix, R. J. *Surf. Sci.* **1981**, *102*, 542.
(21) Bowker, M.; Madix, R. J. *Vacuum* **1981**, *31*, 711.
(22) Barteau, M. A.; Madix, R. J. *Surf. Sci.* **1982**, *115*, 355.
(23) Klink, C.; Stensgaard, I.; Besenbacher, F.; Laegsgaard, E. *Surf. Sci.* **1996**, *360*, 171.
(24) Umbach, E.; Fuggle, J. C.; Menzel, D. *J. Electron Spectrosc. Relat. Phenom.* **1977**, *10*, 15.
(25) Brundle, C. R.; Wandelt, K. In *Proceedings of the 7th International Vacuum Congress and the 3rd International Conference on Solid Surfaces*, Vienna, 1977; p 1173.
(26) Fuggle, J. C.; Menzel, D. In *Proceedings of the 7th International Vacuum Congress and the 3rd International Conference on Solid Surfaces*, Vienna, 1977; p 1003.
(27) Fuggle, J. C.; Umbach, E.; Menzel, D.; Wandelt, K.; Brundle, C. R. *Solid State Commun.* **1978**, *27*, 65.
(28) Alemozafar, A. R.; Madix, R. J. Submitted 2003.
(29) Alemozafar, A. R.; Guo, X.-C.; Madix, R. J. *Surf. Sci.* **2003**, *524* (1−3), L84.
(30) Guo, X.-C.; Madix, R. J. *Surf. Sci.* In Press 2002.
(31) Alemozafar, A. R.; Guo, X.-C.; Madix, R. J. *J. Chem. Phys.* **2002**, *116*, 4698.
(32) Guo, X.-C.; Madix, R. J. *Surf. Sci.* **2002**, *501*, 37.
(33) Alemozafar, A. R.; Guo, X.-C.; Madix, R. J.; Hartmann, N.; Wang, J. *Surf. Sci.* **2002**, *504*, 223.
(34) Somorjai, G.; Ruprechter, G. *J. Chem. Educ.* **1998**, *75*, 161.
(35) Silva, S. L.; Patel, A. A.; Pham, T. M.; Leibsle, F. M. *Surf. Sci.* **1999**, *441*, 351.
(36) Leibsle, F. M.; Haq, S.; Frederick, B. G.; Bowker, M.; Richardson, N. V. *Surf. Sci.* **1995**, *343*, L1175.
(37) Haq, S.; Leibsle, F. M. *Surf. Sci.* **1996**, *355*, L345.
(38) Eierdal, L.; Besenbacher, F.; Lægsgaard, E.; Stensgaard, I. *Surf. Sci.* **1994**, *312*, 31.
(39) Alemozafar, A. R.; Madix, R. J. Submitted 2003.